Na^+-Pyrophosphatase: A Novel Primary Sodium Pump†

Anssi M. Malinen,‡ Georgiy A. Belogurov,‡,|| Alexander A. Baykov,*,§ and Reijo Lahti*,‡

Department of Biochemistry and Food Chemistry, University of Turku, FIN-20014 Turku, Finland, and A. N. Belozersky Institute of Physico-Chemical Biology, Moscow State University, Moscow 119899, Russia

Received March 23, 2007; Revised Manuscript Received May 24, 2007

ABSTRACT: Membrane-bound pyrophosphatase (PPase) is commonly believed to couple pyrophosphate (PP_i) hydrolysis to H^+ transport across the membrane. Here, we demonstrate that two newly isolated bacterial membrane PPases from the mesophile *Methanosarcina mazei* (Mm-PPase) and the moderate thermophile *Moorella thermoacetica* and a previously described PPase from the hyperthermophilic bacterium *Thermotoga maritima* catalyze Na^+ rather than H^+ transport into *Escherichia coli* inner membrane vesicles (IMV). When assayed in uncoupled IMV, the three PPases exhibit an absolute requirement for Na^+ but display the highest hydrolyzing activity in the presence of both Na^+ and K^+. Steady-state kinetic analysis of PP_i hydrolysis by Mm-PPase revealed two Na^+ binding sites. One of these sites can also bind K^+, resulting in a 10-fold increase in the affinity of the other site for Na^+ and a 2-fold increase in maximal velocity. PP_i-driven $^{22}Na^+$ transport into IMV containing Mm-PPase was unaffected by the protonophore carbonyl cyanide *m*-chlorophenylhydrazone, inhibited by the Na^+ ionophore monensin, and activated by the K^+ ionophore valinomycin. The Na^+ transport was accompanied by the generation of a positive inside membrane potential as reported by Oxonol VI. These findings define Na^+-dependent PPases as electrogenic Na^+ pumps. Phylogenetic analysis suggests that ancient gene duplication preceded the split of Na^+- and H^+-PPases.

Membrane pyrophosphatases (PPases[1], EC 3.6.1.1) are integral membrane proteins commonly found in the cytoplasmic membrane of diverse bacteria and archaea, whereas in plants and protozoa, they are located in vacuoles and acidocalcisomes (*1*−*4*). Membrane PPases isolated from several sources have been shown to couple pyrophosphate (PP_i) hydrolysis to the transmembrane transport of protons against an electrochemical potential gradient (*4*−*6*). Accordingly, this enzyme is often called H^+-PPase by analogy with H^+-ATPase. H^+-PPases represent a distinct class of ion translocases that do not have sequence homology to ubiquitous ATP-energized pumps, including F-, V- and P-type ATPases and ABC transporters (*7*). In H^+-PPases, the substrate-binding domain faces the cytoplasm, and the direction of proton pumping is away from the cytoplasm.

In plants, in addition to acidifying the vacuole, H^+-PPase activity facilitates auxin transport. Consequently, the loss of H^+-PPase function in *Arabidopsis thaliana* causes severely disturbed organ development, whereas up-regulation of H^+-PPase promotes root and shoot growth (*8*). The latter effect renders the host plant (e.g., tomato or tobacco) more tolerant to salt and drought (*9*−*11*), making H^+-PPase a valuable tool for crop engineering. In bacteria, H^+-PPase contributes to stress resistance by providing essential energy reserves during metabolic transitions and low-energy conditions (*12*, *13*).

Although all membrane PPases have an absolute requirement for Mg^{2+}, their requirements for alkali cations differ. Specifically, K^+-independent and -dependent subfamilies of H^+-PPases have been previously identified (*6*, *14*, *15*). Both subfamilies occur in bacteria and archaea, whereas plant PPases usually belong to the K^+-dependent subfamily. The subfamilies are clearly homologous but differ in that alkali-cation independent PPases contain Lys, and K^+-dependent PPases contain Ala in the GNXX(K/A) signature sequence (*15*). Furthermore, we recently discovered that the hyperthermophilic bacterium *Thermotoga maritima* contains an evolutionarily related Na^+-dependent membrane PPase (Tm-PPase) (*16*). The absolute requirement of Tm-PPase for Na^+ raised the possibility that it could function as a PP_i-energized Na^+ transporter in *T. maritima*. However, this possibility could not be easily tested in a natural or reconstituted system because the activity of this thermophilic enzyme was too low at temperatures compatible with membrane vesicle integrity. Because we were unsure whether Tm-PPase was

† This work was supported by grants from the Academy of Finland (no. 201611 and 114706), the Ministry of Education and the Academy of Finland (for the National Graduate School in Informational and Structural Biology), and the Russian Foundation for Basic Research (no. 06-04-48887).

* To whom correspondence may be addressed. Tel: 358-2-333-6845. Fax: 358-2-333-6860. E-mail: reijo.lahti@utu.fi (R.L.). Tel: 7-495-939-5541. Fax: 7-495-939-3181. E-mail: baykov@genebee.msu.su (A.B.).

‡ University of Turku.

§ Moscow State University.

|| Current address: Department of Microbiology and The RNA Group, The Ohio State University, 484 West 12th Avenue, Columbus, OH 43210.

[1] Abbreviations: CCCP, carbonyl cyanide *m*-chlorophenylhydrazone; EGTA, ethylene glycol bis(2-aminoethyl ether)-*N*,*N*,*N*′*N*′-tetraacetic acid; IMV, inner membrane vesicles; MES, 2-(*N*-morpholino)ethanesulfonic acid; MOPS, 3-(*N*-morpholino)propanesulfonic acid; Mm-PPase, *Methanosarcina mazei* pyrophosphatase; Mt-PPase, *Moorella thermoacetica* pyrophosphatase; PPase, pyrophosphatase; R-PPase, *Rhodospirillum rubrum* pyrophosphatase; TAPS, 3-{[2-hydroxy-1,1-bis(hydroxymethyl)ethyl]amino}-1-propanesulfonic acid; TMA, tetramethylammonium; Tm-PPase, *Thermotoga maritima* pyrophosphatase.

10.1021/bi700564b CCC: $37.00
Published on Web 07/03/2007

a curious rarity or the first member of a previously unrecognized subfamily of Na^+-dependent PPases, we undertook a search for Na^+-dependent PPases from other bacteria, including mesophilic sources. In the present article, we describe two more Na^+-dependent PPases and show that they do translocate Na^+ instead of H^+ across the membrane.

EXPERIMENTAL PROCEDURES

Plasmid Construction. The *Methanosarcina mazei* PPase (Mm-PPase) gene (GenBank protein accession number NP_632724) (*17*) and *Moorella thermoacetica* PPase (Mt-PPase) gene (GenBank protein accession number YP_430205) were amplified from genomic DNAs (DSMZ) by PCR using *Pfu*-Turbo DNA polymerase (Stratagene). In the case of Mm-PPase, the primers incorporated artificial *Nco*I and *Xho*I restriction sites. The PCR products were digested with *NcoI* and *Xho*I and inserted into the multiple cloning site of pET15b(+) (Novagen). The Mm-PPase gene was then subcloned to pET36(+) (Novagen) using *Xba*I and *Xho*I restriction sites. The resulting construct was named Maz-pET. In the case of Mt-PPase, primers incorporating artificial *Nde*I and *Xho*I restriction sites were employed. The PCR products were digested with *NdeI* and *Xho*I and inserted into the multiple cloning site of pET36b(+) (Novagen). The resulting construct was named Moo-pET.

To improve the expression yield, constructs with modified N-termini were also generated. For the MazM-pET construct, the N-terminal sequence MEMLI of Mm-PPase was replaced with the sequence MLI by inverse PCR using primers 5′-ATGTTAATCTACCTTACACCAATATGTGCC-3′ and 5′-GGTATATCTCCTTCTTAAAGTTAAAC-3′ and Maz-pET as the template. For the MooM-pET construct, the N-terminal sequence MELLAPLTGIV of Mt-PPase was similarly replaced by the sequence MIIYLAPLAGIV using primers 5′-ATTATTTATTTAGCACCACTGGCAGGGATAGTGG-CCTTGCTTTTTGCC-3′ and 5′-CATATGTATATCTCCT-TCTTAAAGTTAAAC-3′ and Moo-pET as the template. The PPase-encoding regions of the constructs were sequenced to confirm the absence of secondary substitutions. Making the N-termini of Mm-PPase and Mt-PPase more hydrophobic appeared to facilitate their insertion into the membrane, increasing the activity yield by factors of 2 and 10, respectively. The N-terminally modified PPases were used in transport studies, whereas the authentic PPases were employed in PP_i hydrolysis studies.

Western Analysis. IMV were diluted ~500-fold with sample buffer (63 mM Tris-HCl at pH 6.8, 10% glycerol, 1% SDS, and 300 mM dithiothreitol). The mixture was heated for 5 min at 95 °C, and then 0.2 μg of protein (in 5 μL total volume) from each sample was electrophoresed on a 12% polyacrylamide gel containing 0.1% SDS (*18*). The resolved samples were transferred to a nitrocellulose Hybond ECL membrane (GE Healthcare) in standard Towbin buffer (*19*) containing 20% (v/v) methanol for 1 h at 100 V in a Mini-PROTEAN 3 apparatus (Bio-Rad). The membrane was blocked in 5% fat-free milk in TBS buffer (20 mM Tris-HCl at pH 7.6, 50 mM NaCl, and 0.2% *n*-dodecyl-β-D-maltoside). Rabbit antiserum raised against the peptide IYTKAADVGADLVGKVE, which is conserved in membrane PPases (MedProbe), was diluted 10000-fold in TBS buffer and allowed to bind for 1 h at room temperature. A peroxidase-labeled secondary antibody and an ECL kit (GE Healthcare) were used to visualize the PPase antiserum-reactive bands.

Enzyme Expression and Vesicle Isolation. PPases were expressed in *Escherichia coli* C41 (DE3) cells (*20*) bearing an additional pAYCA-RIL plasmid (Stratagene), which supplies tRNAs for codons that are rare in *E. coli*. Inverted membrane vesicles (IMV) were prepared by a French press method and isolated by a two-step ultracentrifugation procedure as described previously for *T. maritima* PPase (*16*). The IMV used in transport studies were subjected to a third ultracentrifugation step in storage buffer (10 mM MOPS-tetramethylammonium (TMA) hydroxide at pH 7.2, 150 mM sucrose, 1 mM $MgCl_2$, and 40 μM EGTA) to reduce the sucrose concentration. The membrane pellet was suspended in storage buffer, frozen in liquid N_2, and stored at −70 °C. The amounts of *E. coli* IMV were calculated according to their protein content, which was estimated using the Bradford assay (*21*).

PP_i Hydrolysis Assay. Because *E. coli* lacks endogenous membrane-bound PPases and because the IMV isolation protocol efficiently washes away soluble *E. coli* PPases (<2% background PPase activity remaining), the IMV prepared from the cells bearing PPase expression plasmids can be used directly for activity measurements. The reaction medium, in an initial volume of 25 mL, typically included 0.1 M MOPS-TMA hydroxide (pH 7.2), 5.3 mM $MgCl_2$, 50 μM EGTA, 5−50 μL of IMV suspension (0.05−0.5 mg protein), and various concentrations of NaCl and KCl. IMV were preincubated in this reaction medium for 1 min at 40 °C, and the reaction was initiated by the addition of 160 μM TMA_4-PP_i (giving 100 μM Mg_2PP_i complex). Liberation of inorganic phosphate was continuously recorded for ~3 min with an automatic inorganic phosphate analyzer (*22*). The results of duplicate measurements agreed within 10%. Control experiments using TMA chloride instead of NaCl and KCl indicated that the ionic strength did not significantly affect activity. Established Na^+- and K^+-free reagents (<10 μM Na^+ or K^+) (*16*) were employed to assess the dependence of catalysis on Na^+ and K^+. The concentrations of contaminating Na^+ and K^+ ions in the assay medium were estimated using a SpectrAA-300 atomic absorption spectrometer (Varian Techtron). The buffers used in pH dependence studies were 0.1 M MES (pH 5.0−6.5), MOPS (pH 6.5−8.0), or TAPS (pH 8.0−10.0), adjusted to the desired pH with TMA hydroxide. These studies were performed at saturating concentrations of metal cofactors (20 mM $MgCl_2$, 50 mM KCl, and 20 mM NaCl at pH ≤5.5 or 10 mM NaCl at pH >5.5). Under all conditions tested, the concentration of Mg_2PP_i (100 μM) was saturating. The amounts of PP_i required to maintain this concentration of Mg_2PP_i complex at various pH values were calculated as described previously using the dissociation constants for the Mg^{2+}, K^+, and H^+ complexes of PP_i (*23*).

Transport Assays. PP_i-energized proton transport into membrane vesicles was assayed by measuring the fluorescence quenching of the pH-sensitive probe acridine orange (*24*). The membrane vesicles were incubated for 2 min in buffer H (20 mM MES-TMA hydroxide (pH 5.5), 20 mM MOPS-TMA hydroxide (pH 7.2), or 20 mM TAPS-TMA hydroxide (pH 9.0) with 0.15 M sucrose, 5 mM $MgCl_2$, 50 mM KCl, 10 mM NaCl, and 10−100 μM EGTA) and

Scheme 1: Na^+ and K^+ Activation of Mm-PPase

$$\begin{array}{ccccccc} & & K_{Na1(K)} & & V_1 & & \\ \mathbf{EK} & \leftrightarrow & \mathbf{EKNa} & \rightarrow & & & \\ \updownarrow K_K & & & & & & \\ & & K_{Na1} & & K_{Na2} & & V_2 \\ \mathbf{E} & \leftrightarrow & \mathbf{ENa} & \leftrightarrow & \mathbf{ENa_2} & \rightarrow & \end{array}$$

4 μM acridine orange at 25 °C, and the reaction was initiated by the addition of 1.9 mM (at pH 5.5; yielding 50 μM Mg_2PP_i), 0.16 mM (at pH 7.2; yielding 100 μM Mg_2PP_i), or 0.14 mM (at pH 9.0; yielding 100 μM Mg_2PP_i) TMA_4-PP_i.

PP_i-energized sodium transport into membrane vesicles was assayed at 0 or 25 °C by following the accumulation of $^{22}Na^+$ in the vesicles using a modification of a previously described procedure (*25*). The vesicles were preincubated in 0.7 mL of buffer NS (0.1 M MOPS-TMA hydroxide at pH 7.2, 0.15 M sucrose, 5 mM $MgSO_4$, 25 mM K_2SO_4, 0.5 mM Na_2SO_4, and 50 μM EGTA) or buffer NC (0.1 M MOPS-TMA hydroxide at pH 7.2, 0.15 M sucrose, 5 mM $MgCl_2$, 50 mM KCl, 1 mM NaCl, and 50 μM EGTA) including ~0.3 μCi of ^{22}NaCl (carrier-free, Perkin-Elmer) for ~2 h at the assay temperature. The reaction was started by adding 0.9 mM TMA_4-PP_i. Aliquots (80 μL) were withdrawn at appropriate times and rapidly (<10 s) passed through Dowex 50 ion exchange columns (5 × 12 mm). The columns were washed with 0.5 mL of 0.1 M MOPS-TMA hydroxide at pH 7.2, 150 mM sucrose, 5 mM $MgCl_2$, 10 mM KCl, and 50 μM EGTA. The eluate contained the IMV, whereas all external $^{22}Na^+$ remained bound to the column. The amount of $^{22}Na^+$ in the IMV was determined by liquid scintillation counting.

The generation of a membrane potential was detected as a red shift in the absorbance maximum of Oxonol VI (Invitrogen) (*26*). IMV (1.1 mg/mL) were incubated in buffer NS supplemented with 2 μM Oxonol VI for 2 h, and the reaction was started by adding 1 mM TMA_4-PP_i. The absorbance spectra were recorded with an LKB Biochrom 4060 UV−VIS spectrophotometer (Pharmacia).

Data Analysis. The dependence of the hydrolytic activity of Mm-PPase on Na^+ and K^+ concentrations at saturating substrate and Mg^{2+} concentrations was interpreted using the kinetic model shown in Scheme 1. Scheme 1 involves two parallel routes, one for the K^+-free enzyme and the other for the K^+-bound enzyme, and implies the presence of at least two activating binding sites for alkali cations on Mm-PPase. The corresponding rate equation (eq 1), derived assuming equilibrium binding of Na^+ and K^+, includes two maximal velocities (V_1 for Na^+- and K^+-activated enzyme; V_2 for sodium-activated enzyme) and four equilibrium constants governing the binding of Na^+ to the K^+-free enzyme (K_{Na1} and K_{Na2},) or to the K^+-bound enzyme ($K_{Na1(K)}$), or K^+ binding to the Na^+-free enzyme (K_K):

$$v = v_0 + (V_1[Na][K]/K_K K_{Na1(K)} + V_2[Na]^2/K_{Na1}K_{Na2})/(1 + [Na]/K_{Na1} + [K]/K_K + [Na]^2/K_{Na1}K_{Na2} + [Na][K]/K_K K_{Na1(K)}) \quad (1)$$

Parameter v_o is the basal activity of IMV due to contaminating *E. coli* PPase that is insensitive to Na^+ and K^+.

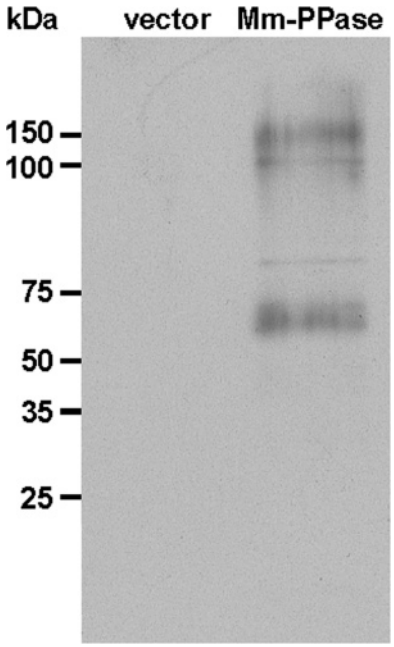

FIGURE 1: Western analysis of IMV prepared from C41(DE3) cells expressing Mm-PPase or transformed with vector only. IMV (0.2 μg) was subjected to SDS−PAGE, electrotransferred and probed with PPase polyclonal antiserum.

Numerical values for all parameters were determined by fitting eq 1 to the rate data using SCIENTIST software (MicroMath). Rate values were weighted according to $1/v^2$.

RESULTS

Mm-PPase is Functionally Expressed in E. coli. The *M. mazei* membrane PPase was expressed in *E. coli* C41 (DE3) cells (*20*), and IMV were isolated using the method previously established for bacterial membrane PPases (*15*, *16*, *24*). Western blot analysis of IMV using a rabbit antiserum raised against the conserved peptide in membrane PPases, IYTKAADVGADLVGKVE, which is conserved in membrane PPases (MedProbe), revealed major ~70 and ~140 kDa bands, which correspond to the calculated molecular masses of monomeric (69.0 kDa) and dimeric Mm-PPase, respectively (Figure 1). No immunoreactive protein was present in the authentic *E. coli* IMV. The PPase activity of the Mm-PPase IMV measured in the presence of 50 mM K^+ and 10 mM Na^+ at 40 °C was 2.2 μmol min^{-1} mg^{-1}, which exceeded the value of 0.4 μmol min^{-1} mg^{-1} reported for Tm-PPase IMV, wherein PPase accounted for 2% of the total protein (*16*). The activity of the Mm-PPase IMV displayed typical properties of a membrane PPase, such as low sensitivity to the soluble PPase inhibitor fluoride (5% inhibition at 0.25 mM), hypersensitivity to the membrane PPase inhibitor aminomethylenediphosphonate (>95% inhibition at 20 μM), and an absolute dependence on Mg^{2+} for activity. The expressed gene thus encodes a functional membrane PPase.

Mm-PPase Requires Na^+ for Activity. In the absence of Na^+, Mm-PPase activity was indistinguishable from the background over the entire range of K^+ concentrations examined (0−100 mM). As the concentration of Na^+ was raised, the PPase activity increased up to a plateau level (Figure 2A). Increasing the K^+ concentration progressively shifted the Na^+ dose−response curve to lower concentrations

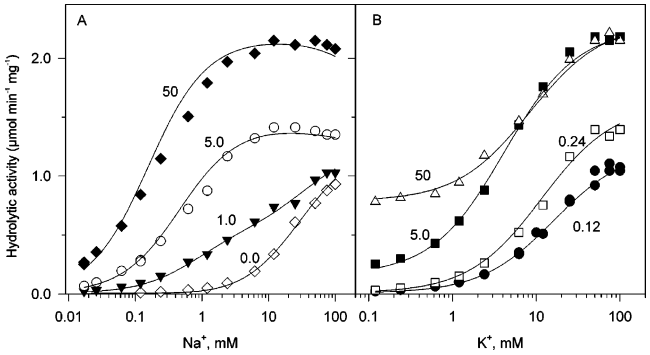

FIGURE 2: Dependence of the rate of PP_i hydrolysis by Mm-PPase IMV on Na^+ and K^+ at 40 °C. Numbers on the curves show fixed K^+ (A) or Na^+ (B) concentrations in millimolar. The lines were drawn according to eq 1 using parameter values found in Table 1.

Table 1: Kinetic Parameters for Scheme 1

parameter	value
V_1 (μmol min^{-1} mg^{-1})	2.30 ± 0.03
V_2 (μmol min^{-1} mg^{-1})	1.25 ± 0.04
v_0 (μmol min^{-1} mg^{-1})	0.005 ± 0.001
K_{Na1} (mM)	1.04 ± 0.08
K_{Na2} (mM)	30 ± 3
K_K (mM)	31 ± 3
$K_{Na1(K)}$ (mM)	0.104 ± 0.006

(i.e., to the left) and increased the maximum activity. In the presence of Na^+, the activity increased with increasing K^+ concentrations (Figure 2B). These results indicated that Mm-PPase absolutely requires Na^+ for activity, whereas both Na^+ and K^+ are needed for maximal activity. Rb^+ could substitute for K^+ but not Na^+ as an activator of Mm-PPase and was effective in the same concentration range.

Quantitative analysis of these data also indicated that Mm-PPase closely resembles Tm-PPase in its alkali cation requirement. The dependence of Mm-PPase activity on the concentration of alkali cations could be described by a simple model, implying the presence of two alkali cation binding sites on the enzyme (Scheme 1). This model is a simplified version of that for Tm-PPase (*16*). Although both models involve two parallel routes, one for K^+-free enzyme and the other for K^+-bound enzyme, the number of the essential Na^+ ions in the K^+-dependent route is reduced by one in Scheme 1, and it does not incorporate inhibition by excess of Na^+ because such inhibition is not observed with Mm-PPase. Accordingly, Scheme 1 contains only five enzyme species, which is three less than the corresponding scheme for Tm-PPase (*16*). This is the simplest model because omitting any species resulted in a significantly poorer fit, whereas adding additional species did not significantly affect the fit.

The parameters describing Scheme 1 were determined by fitting eq 1, derived from Scheme 1, to the rate data and are listed in Table 1. The simplest interpretation is that both the high-affinity site that is highly specific for Na^+ and the low-affinity site that binds both Na^+ and K^+ must be occupied for the enzyme to be active. As evident in Table 1, K^+ increases the affinity of Mm-PPase for Na^+ ~10-fold (K_{Na1} vs $K_{Na(K)}$). Likewise, Na^+ increases the affinity of Mm-PPase for K^+ ~10-fold (K_K vs $K_K K_{Na1(K)}/K_{Na1}$). In addition, the EKNa species is nearly twice as active as the ENa_2 species. Given that bacterial cytoplasm usually contains 10-fold more K^+ than Na^+, the catalytically active complex containing K^+ is likely the most prevalent enzyme species under physiological conditions.

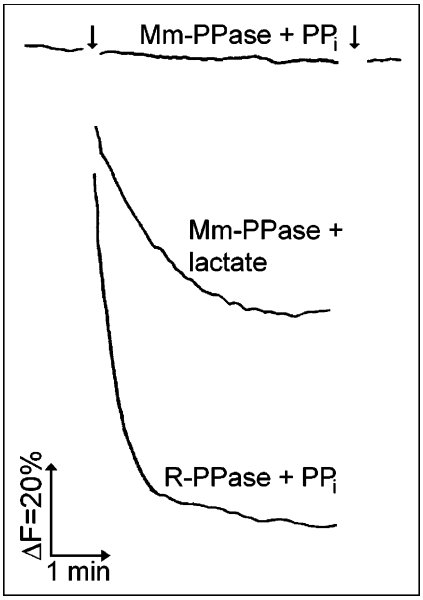

FIGURE 3: H^+ translocation into IMV containing R-PPase (43 μg/mL) or Mm-PPase (55 μg/mL) at pH 7.2 and 25 °C. The left arrow indicates the addition of PP_i or lactate, and the right arrow indicates the addition of 10 mM NH_4Cl to dissipate the H^+ concentration gradient.

The hydrolytic activity of Mm-PPase retained a requirement for Na^+ over a pH range from 5.0 to 10.0. The pH profile at saturating concentrations of Na^+, K^+, Mg^{2+}, and PP_i was bell-shaped, with maximum activity at pH 7.5, indicating the involvement of two ionizable groups with pK_a values of 5.6 ± 0.1 and 9.3 ± 0.1.

Mm-PPase Does Not Pump Protons. We compared the abilities of Mm-PPase and a proton-translocating H^+-PPase from *Rhodospirillum rubrum* (R-PPase) (*24*) to form a PP_i-energized [H^+] gradient measuring the fluorescence quenching of the pH-sensitive probe acridine orange at 25 °C. At this temperature, *E. coli* IMV are resistant to aggregation, and their passive permeability to H^+ is low. Mm-PPase, in contrast to R-PPase, was unable to mediate detectable fluorescence quenching upon addition of PP_i either at pH 7.2 (Figure 3) or at pH 5.5 and 9 (data not shown), although the hydrolytic activities of the PPases were similar. The integrity of the Mm-PPase IMV used was confirmed by their ability to generate an H^+ gradient upon the addition of lactate, which is oxidized by the coupled action of an endogenous *E. coli* membrane enzyme D-lactate dehydrogenase and the electron-transport chain (*27*). These observations indicate that Mm-PPase does not translocate H^+ across the IMV membrane.

Mm-PPase Is an Electrogenic Na^+ Transporter. The absolute requirement of Mm-PPase activity for Na^+ suggested that this enzyme employs Na^+ instead of H^+ as a coupling ion. We therefore directly examined this possibility using $^{22}Na^+$ in the assay medium combined with the separation of IMV from the assay medium by ion exchange chromatography. We observed the rapid accumulation of $^{22}Na^+$ in Mm-PPase IMV upon the addition of PP_i at 25 °C. To investigate the kinetics of this process, we examined the uptake of $^{22}Na^+$ at 0 °C (Figure 4). Importantly, PP_i-driven Na^+ transport was not observed using authentic *E. coli* IMV,

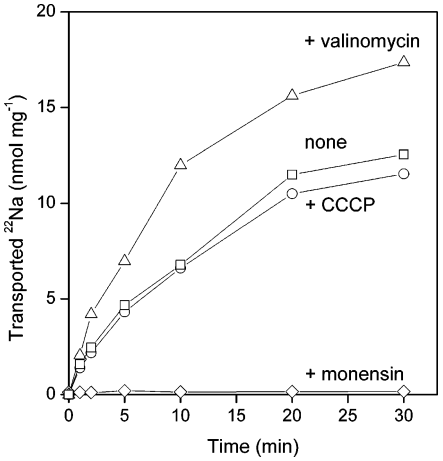

FIGURE 4: PP_i-energized accumulation of $^{22}Na^+$ by Mm-PPase IMV (1.6 mg/mL) at 0 °C. The reaction was started by adding PP_i to the IMV preincubated in buffer NS. Monensin (10 μM), CCCP (20 μM), or valinomycin (2 μM) was included in the preincubation medium as indicated.

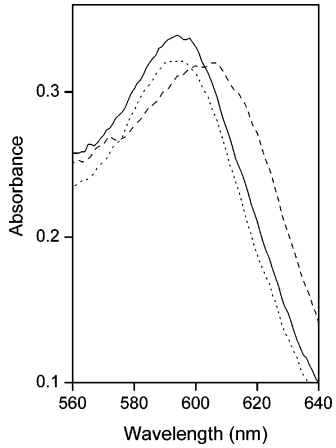

FIGURE 5: Detection of PP_i-induced membrane potential in Mm-PPase IMV by Oxonol VI. The absorbance spectra of Oxonol VI were recorded at 25 °C in buffer NS in resting IMV (—), 0.5 min after the addition of 1 mM TMA_4PP_i (---), and 1 min after the further addition of 2 μM valinomycin to dissipate the membrane potential (···).

which lack membrane PPases, or IMV bearing R-PPase. Monensin, which allows the free diffusion of Na^+ across the membrane, completely prevented the accumulation of $^{22}Na^+$ by the Mm-PPase IMV. Furthermore, adding monensin to IMV preloaded with $^{22}Na^+$ in a 20-min incubation in the presence of PP_i resulted in a rapid (<1 min) and nearly complete loss of the accumulated Na^+. In contrast, the dissipation of any H^+ concentration gradient by the protonophore, carbonyl cyanide *m*-chlorophenylhydrazone (CCCP), did not prevent PP_i-driven $^{22}Na^+$ uptake (Figure 4). Thus, rather than generating a transient H^+ gradient that can be exchanged for Na^+, Mm-PPase directly transports Na^+ across the membrane. The ratios of the initial velocities of PP_i hydrolysis and Na^+ transport were high and variable (3 to 10) in different IMV preparations, and may be attributed to a significant proportion of leaky or uncoupled vesicles, as commonly observed in crude membrane preparations (e.g., ref *25*).

With membrane-impermeable SO_4^{2-} as the only anion in the $^{22}Na^+$ uptake assay buffer (Figure 4), Na^+ transport by Mm-PPase should create a positive inside membrane potential in the IMV unless a charge-balancing cation antiport or anion symport is mechanistically linked to the Na^+ transport activity. We therefore examined the formation of a membrane potential using two different methods. First, we found that valinomycin, which allows free diffusion of K^+ across the membrane and thus dissipates any formed membrane potential, increased the initial rate of $^{22}Na^+$ transport and the final amount of $^{22}Na^+$ accumulated (Figure 4). In a set of 22 independent measurements, valinomycin enhanced Na^+ accumulation in 30 min by 33 ± 10% (SD). Second, we found that Na^+ transport resulted in a red shift in the absorbance maximum (from 595 to 605 nm) of the optical membrane potential probe Oxonol VI (Figure 5), indicating the formation of a positive inside potential. The absorbance maximum reverted when the membrane potential was dissipated by the addition of valinomycin. Together, this evidence suggests that Mm-PPase is an electrogenic Na^+ transporter; however, the quantitative estimation of the membrane potential should await experiments with better sealed and more uniform membrane preparations.

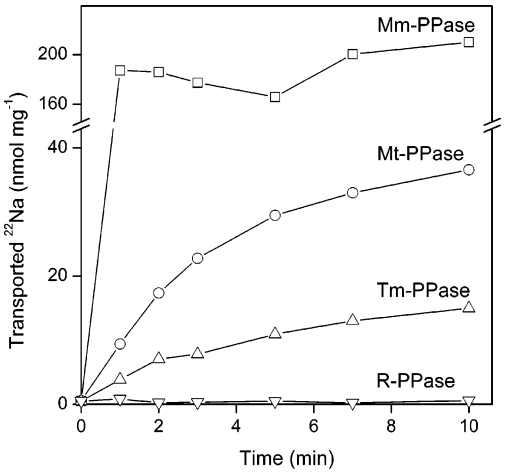

FIGURE 6: PP_i-energized accumulation of $^{22}Na^+$ by IMV harboring Mm-PPase (0.4 mg/mL), Mt-PPase (2.4 mg/mL), Tm-PPase (3.2 mg/mL), or R-PPase (0.5 mg/mL) at 25 °C in buffer NC.

Several lines of evidence indicate that Na^+ transport into IMV builds up a Na^+ concentration gradient (higher concentration inside), rather than merely allowing equilibration of the ion across the membrane. First, the maximal amount of Na^+ accumulated by *M. thermoacetica* IMV increased nearly 10-fold, rather than remaining constant, when temperature was increased from 0 °C (Figure 4) to 25 °C (Figure 6). Second, no significant change (<10%) in the maximal amount of accumulated Na^+ was observed when Na^+ concentration in the assay medium was decreased to 0.5 mM or increased to 2 mM (data not shown). Of note, the hydrolytic and pumping activities were stimulated at the increased temperature but were independent of $[Na^+]$ in the range tested (Figure 2). Third, depletion of PP_i from the incubation medium, by the addition of 17 μM *E. coli* soluble PPase to IMV preloaded with Na^+ as in Figure 6, caused efflux of Na^+ that was complete in 60 min.

Because the effect of Rb^+ on Mm-PPase activity was similar to that of K^+, we examined the possible transport of Rb^+ into or out of IMV by performing a transport assay using $^{86}Rb^+$ in place of K^+. Following a 2-h equilibration of non-energized IMV with 10 mM $^{86}Rb^+$, 10 mM Na^+, and 20 μM CCCP, addition of PP_i did not induce changes in the

equilibrium concentration of $^{86}Rb^+$ inside IMV in response to Na^+ accumulation at either 0 or 25 °C. Notably, Mm-PPase was able to catalyze PP_i-dependent $^{22}Na^+$ accumulation into IMV in the K^+-free medium. These results collectively indicate that this enzyme is unlikely to transport Rb^+ and its analogue, K^+, together with or in exchange for Na^+ and that Rb^+ and K^+ are not required for the Na^+ transport activity of Mm-PPase.

Na^+-Transporting PPases Are Widespread among Microbes. In addition to Mm-PPase, we identified a membrane PPase from the moderate thermophile *M. thermoacetica* (Mt-PPase) and isolated it in *E. coli* IMV. The hydrolytic activity of Mt-PPase was also strictly dependent on Na^+, and the maximal activity was attained in the presence of both Na^+ and K^+. Moreover, using the sensitive $^{22}Na^+$ transport assay optimized with the mesophilic Mm-PPase, we found that both Mt-PPase and a previously described PPase from the thermophilic marine bacterium *T. maritima* (Tm-PPase) (*16*) catalyze PP_i-driven Na^+ transport into IMV (Figure 6). The transport rates for the thermophilic PPases were lower because the assay temperature (25 °C) was far below the temperatures optimal for enzyme activity. Even with the most thermophilic Tm-PPase, however, the rate was at least 10-fold higher than the R-PPase background. The discovery of Na^+-translocating PPases from three evolutionary and ecologically distant species suggests that many microbes utilize Na^+-transporting PPases.

DISCUSSION

We recently showed that the hyperthermophilic bacterium *T. maritima* contains a novel, Na^+-dependent membrane-bound PPase (*16*). Here, we extend this work by identifying Na^+-dependent PPases in two more microbes, including the mesophile *M. mazei*, and show that the new PPases belong to a previously unknown type of primary Na^+ transporters, the Na^+-translocating PPases. On the basis of phylogenetic analysis of protein sequences (Supporting Information, Figure S1) and the absence of lysine in the GNXX(K/A) signature sequence, these three transporters belong to the subfamily of K^+-dependent PPases (*15*). Consistent with this assignment, Na^+-PPases display maximal activity in the presence of both Na^+ and K^+.

Kinetic analysis of PP_i hydrolysis by Mm-PPase and Mt-PPase suggests that binding of alkali cations to two distinct sites is required for enzyme activity. The higher affinity site is Na^+-specific, likely representing the acceptor site for transported Na^+, and may therefore correspond to the H^+ acceptor site in H^+-PPases. The lower affinity site binds K^+ and Na^+ with similar affinities and is probably the counterpart of the cytoplasmically oriented K^+-binding site in K^+-dependent H^+-PPases (*28*). This site likely serves a regulatory role in both Na^+-translocating PPases and K^+-dependent H^+-translocating PPases and is not directly involved in the transport process. These conclusions are based on the documented failure to detect outwardly directed K^+ transport by H^+-PPases (*29*, *30*) or Rb^+ transport by Na^+-PPases (present study) and the ability of a nontransportable NH_3^+ group introduced by Ala460Lys substitution to eliminate the K^+ dependence of the H^+-PPase of *Carboxydothermus hydrogenoformans* (*15*).

Na^+-PPases appear to be highly specific with respect to the transported ion, and unlike other membrane PPases, they have no H^+-transport activity. Whereas Na^+,K^+-ATPase (*31*) and Na^+-translocating F_1F_0-ATPase (*32*) are able to transport H^+ under low Na^+ or high H^+ concentrations, we did not observe the translocation of H^+ by Na^+-PPase at pH values from 5.5 to 9.0, and the hydrolytic activity retained its Na^+ requirement over a pH range from 5.0 to 10.0. However, identification of further Na^+-PPases is required to pinpoint the residues responsible for the coupling ion specificity of Na^+-PPases and to identify amino acid substitutions that could change the transport specificity.

The discovery of Na^+-PPases explains an observation that has long puzzled researchers, specifically that there are two membrane PPase genes in the genomes of several prokaryotic species. Thus, the archaeon *M. mazei* possesses in addition a gene that encodes an alkali cation-independent H^+-PPase (accession number NP_632725) (*33*). In the unrelated eubacterium *M. thermoacetica*, the Na^+-PPase is accompanied by a PPase (accession number YP_429292) that is also classified as an alkali cation-independent H^+-PPase because of the presence of a conserved Lys residue in the GNXX-(K/A) signature sequence. This dichotomy in PPase function is also predicted in *Dehalococcoides ethenogenes* (*34*). Significantly, in *M. mazei*, the Na^+-PPase and H^+-PPase genes are adjacent to each other on the chromosome, suggesting that this gene cluster may be the footprint of an ancient gene duplication that preceded the split of Na^+- and H^+-PPases. The duplication likely involved a K^+-dependent enzyme because the K^+-dependent H^+-PPases are more closely related to the Na^+-PPases than the alkali cation-independent H^+-PPases (Supporting Information, Figure S1). Importantly, the dichotomy in PPase functions was fixed because the change in the transported ion specificity of one of the duplicated gene products allowed the host species to utilize PP_i for the generation of both Na^+ and H^+ gradients across the membrane.

The role of Na^+-PPase can be most easily conjectured in the thermophilic marine bacterium, *T. maritima*, which utilizes Na^+ as the primary bioenergetic coupling ion and employs a Na^+-ATP-synthase (*35*, *36*). In this organism, Na^+-PPase may work in concert with Na^+-ATP-synthase to scavenge energy from biosynthetic waste (PP_i) in order to maintain the Na^+ gradient, especially under energy-limiting conditions. In contrast, both *M. mazei* and *M. thermoacetica* have H^+-coupled ATP synthases (*37*, *38*) and possess genes encoding H^+-PPases. In these organisms, which can grow under conditions of high salinity (up to 1 M NaCl), Na^+-PPase could theoretically replace or work in parallel with the Na^+/H^+ antiporter to maintain low internal Na^+ concentrations. Notably, Na^+-PPase is the first primary Na^+ transporter to be identified in *M. thermoacetica* (*37*, *38*).

In future investigations, it will be interesting to examine whether other members of the large subfamily of K^+-dependent PPases, which includes bacterial and most plant vacuolar PPases, can operate as Na^+ transporters. Such PPases could prove to be valuable tools for the development of salt-resistant bacteria and plants.

SUPPORTING INFORMATION AVAILABLE

Figure S1 (Bayesian estimate of membrane PPase phylogeny). This material is available free of charge via the Internet at http://pubs.acs.org.

REFERENCES

1. Rea, P. A., and Poole, R. J. (1993) Vacuolar H^+-translocating pyrophosphatases, *Annu. Rev. Plant Physiol. Plant Mol. Biol. 44*, 157−180.
2. Serrano, A., Perez-Castineira, J. R., Baltscheffsky, H., and Baltscheffsky, M. (2004) Proton-pumping inorganic pyrophosphatases in some archaea and other extremophilic prokaryotes, *J. Bioenerg. Biomembr. 36*, 127−133.
3. Docampo, R., de Souza, W., Miranda, K., Rohloff, P., and Moreno, S. N. (2005) Acidocalcisomes: conserved from bacteria to man, *Nat. Rev. Microbiol. 3*, 251−261.
4. Maeshima, M. (2000) Vacuolar H^+-pyrophosphatase, *Biochim. Biophys. Acta 1465*, 37−51.
5. Baltscheffsky, M., Schultz, A., and Baltscheffsky, H. (1999) H^+-PPases: a tightly membrane-bound family, *FEBS Lett. 457*, 527−533.
6. Drozdowicz, Y. M., and Rea, P. A. (2001) Vacuolar H^+ pyrophosphatases: from the evolutionary backwaters into the mainstream, *Trends Plant Sci. 6*, 206−211.
7. Rea, P. A., Kim, Y., Sarafian, V., Poole, R. J., Davies, J. M., and Sanders, D. (1992) Vacuolar H^+-translocating pyrophosphatases: a new category of ion translocase, *Trends Biochem. Sci. 17*, 348−353.
8. Li, J., Yang, H., Peer, W. A., Richter, G., Blakeslee, J., Bandyopadhyay, A., Titapiwantakun, B., Undurraga, S., Khodakovskaya, M., Richards, E. L., Krizek, B., Murphy, A. S., Gilroy, S., and Gaxiola, R. (2005) Arabidopsis H^+-PPase AVP1 regulates auxin-mediated organ development, *Science 310*, 121−125.
9. Gaxiola, R. A., Li, J., Undurraga, S., Dang, L. M., Allen, G. J., Alper, S. L., and Fink, G. R. (2001) Drought- and salt-tolerant plants result from overexpression of the AVP1 H^+-pump, *Proc. Natl. Acad. Sci. U.S.A. 98*, 11444−11449.
10. Park, S., Li, J., Pittman, J. K., Berkowitz, G. A., Yang, H., Undurraga, S., Morris, J., Hirschi, K. D., and Gaxiola, R. A. (2005) Up-regulation of a H^+-pyrophosphatase (H^+-PPase) as a strategy to engineer drought-resistant crop plants, *Proc. Natl. Acad. Sci. U.S.A. 102*, 18830−18835.
11. Gao, F., Gao, Q., Duan, X., Yue, G., Yang, A., and Zhang, J. (2006) Cloning of an H^+-PPase gene from *Thellungiella halophila* and its heterologous expression to improve tobacco salt tolerance, *J. Exp. Bot. 57*, 3259−3270.
12. Garcia-Contreras, R., Celis, H., and Romero, I. (2004) Importance of *Rhodospirillum rubrum* H^+-pyrophosphatase under low-energy conditions, *J. Bacteriol. 186*, 6651−6655.
13. Lopez-Marques, R. L., Perez-Castineira, J. R., Losada, M., and Serrano, A. (2004) Differential regulation of soluble and membrane-bound inorganic pyrophosphatases in the photosynthetic bacterium *Rhodospirillum rubrum* provides insights into pyrophosphate-based stress bioenergetics, *J. Bacteriol. 186*, 5418−5426.
14. Perez-Castineira, J. R., Lopez-Marques, R. L., Losada, M., and Serrano, A. (2001) A thermostable K^+-stimulated vacuolar-type pyrophosphatase from the hyperthermophilic bacterium *Thermotoga maritima*, *FEBS Lett. 496*, 6−11.
15. Belogurov, G. A., and Lahti, R. (2002) A lysine substitute for K^+. A460K mutation eliminates K^+ dependence in H^+-pyrophosphatase of *Carboxydothermus hydrogenoformans*, *J. Biol. Chem. 277*, 49651−49654.
16. Belogurov, G. A., Malinen, A. M., Turkina, M. V., Jalonen, U., Rytkonen, K., Baykov, A. A., and Lahti, R. (2005) Membrane-bound pyrophosphatase of *Thermotoga maritima* requires sodium for activity, *Biochemistry 44*, 2088−2096.
17. Deppenmeier, U., Johann, A., Hartsch, T., Merkl, R., Schmitz, R. A., Martinez-Arias, R., Henne, A., Wiezer, A., Baumer, S., Jacobi, C., Bruggemann, H., Lienard, T., Christmann, A., Bomeke, M., Steckel, S., Bhattacharyya, A., Lykidis, A., Overbeek, R., Klenk, H. P., Gunsalus, R. P., Fritz, H. J., and Gottschalk, G. (2002) The genome of *Methanosarcina mazei*: evidence for lateral gene transfer between bacteria and archaea, *J. Mol. Microbiol. Biotechnol. 4*, 453−461.
18. Laemmli, U. K. (1970) Cleavage of structural proteins during the assembly of the head of bacteriophage T4, *Nature 227*, 680−685.
19. Towbin, H., Staehelin, T., and Gordon, J. (1979) Electrophoretic transfer of proteins from polyacrylamide gels to nitrocellulose sheets: procedure and some applications, *Proc. Natl. Acad. Sci. U.S.A. 76*, 4350−4354.
20. Miroux, B., and Walker, J. E. (1996) Over-production of proteins in *Escherichia coli*: mutant hosts that allow synthesis of some membrane proteins and globular proteins at high levels, *J. Mol. Biol. 260*, 289−298.
21. Bradford, M. M. (1976) A rapid and sensitive method for the quantitation of microgram quantities of protein utilizing the principle of protein-dye binding, *Anal. Biochem. 72*, 248−254.
22. Baykov, A. A., and Avaeva, S. M. (1981) A simple and sensitive apparatus for continuous monitoring of orthophosphate in the presence of acid-labile compounds, *Anal. Biochem. 116*, 1−4.
23. Baykov, A. A., Bakuleva, N. P., and Rea, P. A. (1993) Steady-state kinetics of substrate hydrolysis by vacuolar H^+-pyrophosphatase. A simple three-state model, *Eur. J. Biochem. 217*, 755−762.
24. Belogurov, G. A., Turkina, M. V., Penttinen, A., Huopalahti, S., Baykov, A. A., and Lahti, R. (2002) H^+-pyrophosphatase of *Rhodospirillum rubrum:* High-yield expression in *Escherichia coli* and identification of the Cys residues responsible for inactivation by mersalyl, *J. Biol. Chem. 277*, 22209−22214.
25. Dimroth, P. (1982) The generation of an electrochemical gradient of sodium ions upon decarboxylation of oxaloacetate by the membrane-bound and Na^+-activated oxaloacetate decarboxylase from *Klebsiella aerogenes*, *Eur. J. Biochem. 121*, 443−449.
26. Waggoner, A. S. (1979) Dye indicators of membrane potential, *Annu. Rev. Biophys. Bioeng. 8*, 47−68.
27. Matsushita, K., and Kaback, H. R. (1986) D-lactate oxidation and generation of the proton electrochemical gradient in membrane vesicles from *Escherichia coli* GR19N and in proteoliposomes reconstituted with purified D-lactate dehydrogenase and cytochrome *c* oxidase, *Biochemistry 25*, 2321−2327.
28. Davies, J. M., Rea, P. A., and Sanders, D. (1991) Vacuolar proton-pumping pyrophosphatase in *Beta vulgaris* shows vectorial activation by potassium, *FEBS Lett. 278*, 66−68.
29. Sato, M. H., Kasahara, M., Ishii, N., Homareda, H., Matsui, H., and Yoshida, M. (1994) Purified vacuolar inorganic pyrophosphatase consisting of a 75-kDa polypeptide can pump H^+ into reconstituted proteoliposomes, *J. Biol. Chem. 269*, 6725−6728.
30. Ros, R., Romieu, C., Gibrat, R., and Grignon, C. (1995) The plant inorganic pyrophosphatase does not transport K^+ in vacuole membrane vesicles multilabeled with fluorescent probes for H^+, K^+, and membrane potential, *J. Biol. Chem. 270*, 4368−4374.
31. Polvani, C., and Blostein, R. (1988) Protons as substitutes for sodium and potassium in the sodium pump reaction, *J. Biol. Chem. 263*, 16757−16763.
32. Laubinger, W., and Dimroth, P. (1989) The sodium ion translocating adenosinetriphosphatase of *Propionigenium modestum* pumps protons at low sodium ion concentrations, *Biochemistry 28*, 7194−7198.
33. Baumer, S., Lentes, S., Gottschalk, G., and Deppenmeier, U. (2002) Identification and analysis of proton-translocating pyrophosphatases in the methanogenic archaeon *Methansarcina mazei*, *Archaea 1*, 1−7.
34. Seshadri, R., Adrian, L., Fouts, D. E., Eisen, J. A., Phillippy, A. M., Methe, B. A., Ward, N. L., Nelson, W. C., Deboy, R. T., Khouri, H. M., Kolonay, J. F., Dodson, R. J., Daugherty, S. C., Brinkac, L. M., Sullivan, S. A., Madupu, R., Nelson, K. E., Kang, K. H., Impraim, M., Tran, K., Robinson, J. M., Forberger, H. A., Fraser, C. M., Zinder, S. H., and Heidelberg, J. F. (2005) Genome sequence of the PCE-dechlorinating bacterium *Dehalococcoides ethenogenes*, *Science 307*, 105−108.
35. Dimroth, P., and Cook, G. M. (2004) Bacterial Na^+- or H^+-coupled ATP synthases operating at low electrochemical potential, *Adv. Microb. Physiol. 49*, 175−218.
36. Hase, C. C., Fedorova, N. D., Galperin, M. Y., and Dibrov, P. A. (2001) Sodium ion cycle in bacterial pathogens: evidence from cross-genome comparisons, *Microbiol. Mol. Biol. Rev. 65*, 353−370.
37. Deppenmeier, U. (2002) The unique biochemistry of methanogenesis, *Prog. Nucleic Acid Res. Mol. Biol. 71*, 223−283.
38. Drake, H. L., and Daniel, S. L. (2004) Physiology of the thermophilic acetogen *Moorella thermoacetica*, *Res. Microbiol. 155*, 869−883.

BI700564B